AIP | Applied Physics Letters

Insight on the ferroelectric properties in a (BiFeO3)2(SrTiO3)4 superlattice from experiment and ab initio calculations

E. Bruyer, A. Sayede, A. Ferri, R. Desfeux, R. V. K. Mangalam, R. Ranjith, and W. Prellier

Citation: Applied Physics Letters **107**, 042904 (2015); doi: 10.1063/1.4927600
View online: http://dx.doi.org/10.1063/1.4927600
View Table of Contents: http://scitation.aip.org/content/aip/journal/apl/107/4?ver=pdfcov
Published by the AIP Publishing

Insight on the ferroelectric properties in a $(BiFeO_3)_2(SrTiO_3)_4$ superlattice from experiment and *ab initio* calculations

E. Bruyer,[1,a)] A. Sayede,[1,a)] A. Ferri,[1] R. Desfeux,[1] R. V. K. Mangalam,[2,b)] R. Ranjith,[2,c)] and W. Prellier[2]
[1]*Université d'Artois, Unité de Catalyse et de Chimie du Solide, CNRS UMR 8181, Faculté des Sciences Jean-Perrin, Rue Jean Souvraz, F-62300 Lens Cedex, France*
[2]*Laboratoire CRISMAT, CNRS UMR 6508, ENSICAEN, 6, Boulevard du Maréchal Juin, 14050 Caen Cedex, France*

(Received 21 April 2015; accepted 18 July 2015; published online 28 July 2015)

Ferroelectric domain properties of a $(BiFeO_3)_2(SrTiO_3)_4$ superlattice were studied by means of piezoresponse force microscopy and density functional theory calculations. A combination of out-of-plane and in-plane piezoresponse force imaging confirms that the ferroelectric domains are oriented along the out-of-plane [001] direction of the film. Density functional theory calculations evidence that this orientation is due to the tetragonal-like structure adopted by the $BiFeO_3$ units inside the superlattice in response to the interfacial strains. In addition, antiferrodistortive rotations of the BO_2 planes within both types of ABO_3 blocks (i.e., $SrTiO_3$ as well as $BiFeO_3$ units) are highlighted. Besides, a much lower coercive voltage is measured on superlattices compared to $BiFeO_3$ single layers, suggesting a more reliable switching capability. The results are expected to enable the design of promising multifunctional oxide superlattices. © *2015 AIP Publishing LLC*.
[http://dx.doi.org/10.1063/1.4927600]

With a high antiferromagnetic Néel temperature ($T_N \sim 643$ K) and a high ferroelectric Curie temperature ($T_C \sim 1098$ K), the multiferroic $BiFeO_3$ (BFO) compound is a very promising candidate for applications at room temperature.[1,2] When grown in thin film, the leakage current density was shown to be relatively high, minimizing the interest of this oxide for integration in (nano)-devices. Nevertheless, combining BFO and $SrTiO_3$ (STO) in a superlattice (SL), the leakage current density of BFO thin films was demonstrated to be reduced by two orders of magnitude at room temperature.[3,4] In addition, using both Out-of-Plane (OP) and In-Plane (IP) Piezoresponse Force Microscopy (PFM) for imaging ferroelectric (FE) domains, a reduction in the domains size and a suppression of the in-plane orientation of domains in $(BFO)_4(STO)_8$ SL, compared to single BFO thin films, was highlighted.[3,5] Such observations were thus suggesting a constrained FE domain orientation along the out-of-plane [001] growth direction of SL. However, no detailed information about the structural properties and symmetry adopted by both the STO and BFO in the SL were evidenced. Nevertheless, reciprocal space maps showed clearly that the whole SL took the same in-plane lattice parameter value of STO (3.905 Å). In addition, no distinctive splitting was observed in the average SL_0 peak, as obtained for BFO thin films with monoclinic structure.

In this paper, we extend this study to a $(BFO)_2(STO)_4$ SL using PFM and Density Functional Theory (DFT) calculations, in order to explain the origin of this peculiar orientation for FE domains in $(BFO)_m(STO)_n$ SLs.

(00l)-oriented $(BFO)_2(STO)_4$ SLs (120 nm-thick) were grown on conductive (00l)-oriented $LaNiO_3$ buffer layer deposited on (001)-oriented STO substrates by pulsed laser deposition.[3,5] The FE domain structure was investigated by using a modified commercial atomic force microscope (AFM, Multimode, Nanoscope V, Bruker) working under environmental conditions. Poling experiments were performed to highlight the local ferroelectricity in the films while local piezoloops were acquired to measure the switching behavior.[6]

The FE domain pattern was investigated by OP-PFM and IP-PFM imaging. As seen in Fig. 1(a), the in-phase OP-PFM image reveals the presence of FE domains with both upward (blue contrast) and downward (red contrast) polarizations. However, the as-grown domains are dominated by the upward polarization state, which suggests a self-polarization effect pointing toward the free surface of the film. On the other hand, no contrast is evidenced on the IP-PFM image, indicating the absence of in-plane oriented domains (Fig. 1(b)). Such phenomenon was already observed in $(BFO)_4(STO)_8$ SLs and in ultrathin single layer and suggests a constrained FE domain orientation along the out-of-plane [001] direction, as well as in ultrathin BFO single layer.[5,7] This also indicates that this $(BFO)_m(STO)_n$ SL crystallizes in a structure with specific symmetry, which leads to an out-of plane polarization vector with respect to the plane of the substrate.

Poling experiments were performed in order to get a better insight on the FE domain polarization switching. In Fig. 1(c) is displayed the OP-PFM phase image after application of -10 V DC bias on the tip over $3 \times 3\ \mu m^2$ and subsequently $+10$ V over inside $1 \times 1\ \mu m^2$ area. Well-defined square and uniform contrast are obtained when the DC

[a)]Also at Université Lille Nord de France, F-59000 Lille, France. Electronic addresses: emilie.bruyer@univ-artois.fr and adlane.sayede@univ-artois.fr
[b)]Current address: Department of Materials Science and Engineering and Materials Research Laboratory, University of Illinois, Urbana-Champaign, Urbana, Illinois 61801, USA.
[c)]Current address: Department of Materials Science and Engineering, Indian Institute of Technology Hyderabad, Ordnance Factory Estate, Yeddumailaram 502205, India.

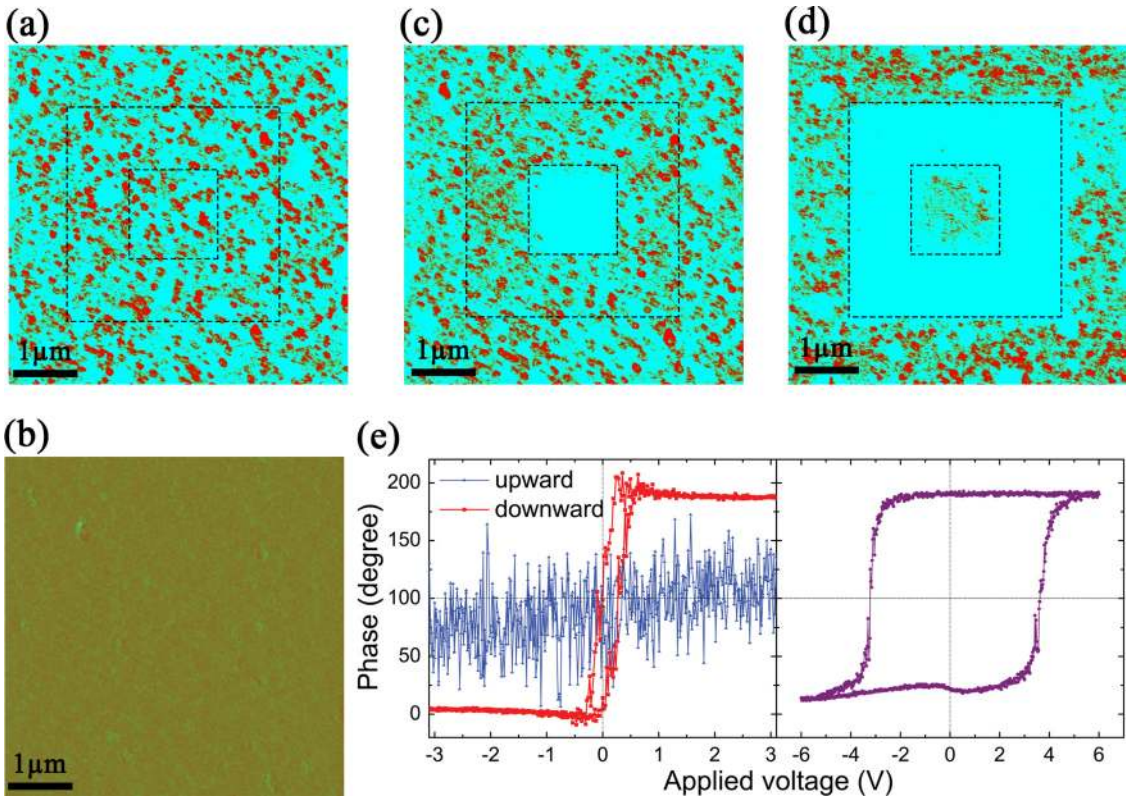

FIG. 1. Images of the (a) OP-PFM and (b) IP-PFM phase signals for the as-grown domains, simultaneously recorded on $(STO)_4(BFO)_2$ SL structure. (c) Corresponding OP-FE domain pattern formed by application of -10 V over $3 \times 3\ \mu m^2$ and subsequently $+10$ V over $1 \times 1\ \mu m^2$. (d) OP-PFM imaging after square areas have been polarized ($3 \times 3\ \mu m^2$) then reverse polarized ($1 \times 1\ \mu m^2$) by applying $+10$ V and subsequently -10 V, respectively. (e) In-phase hysteresis loops measured on downward (red region) and upward (blue region) domains of the $(STO)_4(BFO)_2$ SL (left). In-phase piezoloop of BFO single layer for comparison (right).

voltage of $+10$ V is applied (blue square), suggesting a full switching of domains to upward polarization state. However, no significant change of the phase contrast is observed after applying -10 V DC bias, signifying no switching occurs. This asymmetric switching behavior was confirmed by further polarization switching experiments, where domains were locally manipulated by applying, first, $+10$ V over $3 \times 3\ \mu m^2$ area and second, inside the zone previously manipulated, -10 V over $1 \times 1\ \mu m^2$. Indeed, as illustrated in Fig. 1(d), a uniformly polarized FE region is obtained when a positive voltage is applied to switch up the polarization, while the centered region where the negative bias was applied shows only some red contrast. This indicates the difficulty for upward domains to be switched back into the downward direction. In fact, this polarization imprint phenomenon has been explained by considering the pinning of FE domains at the superlattice-electrode interface.[8,9]

Origins of such switching behavior combined to the upward self-polarization can be a signature of epitaxial strains, strain gradients, charged vacancies, atomic-scale interface, etc.[10,11] In our case, a compressive strain is induced across the $(STO)_4(BFO)_2$ epitaxial SL structure grown on (100)-oriented STO substrate with LNO buffered layer. This epitaxial strain can lead to such a polarization, as previously observed in $BaTiO_3$ or $PbZr_{0.2}Ti_{0.8}O_3$ thin films.[10,12] In addition, considering the n-type LNO metallic oxide used as bottom electrode and the p-type FE SL structure, a p-n junction can be formed in which an internal electric field due to the depletion region induces an upward self-polarization.[8] As a consequence, both the compressive epitaxial strain and the p-n junction may be the main reason of the observed upward ferroelectric self-polarization. Besides, due to the p-n junction, a space-charge region exists at the interface between the LNO bottom electrode and our SL, which can induce domains pinning, as observed in Fig. 1(d).

Local piezoresponse hysteresis loops were measured on the $(STO)_4(BFO)_2$ SL. Fig. 1(e) (left) shows a comparison of the piezoloops measured on downward and upward as-grown domains. A well-defined hysteresis is obtained on downward domains, whereas no PFM signal is detected when an upward domain is probed. This is in agreement with the polarization imprint observed in PFM imaging. From the piezoloop measured on red region, a coercive voltage of about 0.4 V is determined. For comparison, hysteresis loop recorded on a 120 nm-thick BFO single layer grown on similar (100)-STO substrate with LNO as bottom electrode displays a coercive voltage of 3.4 V (Fig. 1(e) (right)). The lower coercive voltage measured on the SL suggests a more reliable switching capability, making such heterostructure more suitable as a functional material for data storage device. This can be directly related to the existence of insulator layers reducing the current leakage into such FE heterostructures, as already observed in similar artificial SL.[3] On the other hand, the FE polarization in BFO thin films is known to be along the pseudo cubic body diagonal $\langle 111 \rangle$, meaning an intermediate direction with respect to the plane and the normal of the substrate. Hence, the DC voltage required for switching FE domains in the film is higher in this latter case compared to a polarization vector normal to the substrate

plane. Such a conclusion was already made for $PbMgNbO_3$-$PbTiO_3$ (PMN-PT) thin films.[6] Furthermore, we note that both piezoloops are shifted toward positive voltage values. According to the loops, shift values of ~0.3 and ~0.2 V are determined for the single layer and the SL, respectively. This phenomenon is characteristic of imprint behavior of the local switching. This is in perfect agreement with the upward self-polarization seen on PFM images. Moreover, we have to keep in mind that such asymmetrical piezoloops in FEs can also be attributed to an internal built-in electric field in the film coming from the asymmetry of the tip/film/bottom electrode configuration.[6,11,13]

In order to get a deeper insight on the internal structure of the $(STO)_4(BFO)_2$ SL, first-principles calculations have been carried out, using the Generalized Gradient Approximation (GGA)+U as implemented in the DFT code VASP.[14] We used the projector augmented wave method[15] by explicitly treating 15 valence electrons for Bi ($5d^{10}6s^26p^3$), 14 for Fe ($3p^63d^64s^2$), 6 for O ($2s^22p^4$), 10 for Sr ($4s^24p^65s^2$), and 12 for Ti ($3s^23p^63d^24s^2$). For all calculations, a 500 eV plane-wave energy cutoff was used, and a criterion of at least 0.01 meV per atom was placed on the self-consistent convergence of the total energy. Integration over the first Brillouin zone was made with a $4 \times 4 \times 1$ Monkhorst-Pack *k*-points mesh centered at Γ. We include an effective Hubbard term $U_{eff} = U–J$ of 4 eV to treat the Fe *3 d* orbitals.[16] We worked with the 120-atom cell depicted in Fig. 2(a), which is obtained by stacking a 80-atom STO and 40-atom BFO cells along the [001] direction. This 120-atom cell is suitable to describe the structural distortions characterizing the low-symmetry phases of many perovskite oxides[17] and hence enables us to explore all the possible octahedral rotational patterns throughout the material. This cell is also well adapted to describe the most relevant antiferromagnetic (AFM) spin arrangements for BFO, i.e., the C-AFM and G-AFM orders. We started our structural analysis by relaxing a BFO/STO stacking where each formula unit of both constituents has initially the ideal cubic perovskite structure (space group $Pm\bar{3}m$, c/a = 1); this structure is labelled as *phase I*. To simulate the growth of such SL onto a (001) STO substrate, we imposed the condition $a = b = a_0(STO)$, where $a_0(STO)$ is the lattice parameter of a cubic unit cell of $SrTiO_3$ after optimization; in our case, we obtained $a_0 = 3.944$ Å, which is comparable to the experimental value (i.e., 3.905 Å), given the slight overestimation (~1%–2%) of lattice parameters usually induced by GGA calculations. The remaining degrees of freedom (namely, the out-of-plane *c* parameter and the internal ionic positions) were optimized by minimizing the Hellman-Feynman forces to a tolerance of 0.005 eV/Å.

In our superlattice, the $SrTiO_3$ (II-IV perovskite) block is made of uncharged SrO and TiO_2 layers, whereas the $BiFeO_3$ (III-III perovskite) block contains charged BiO (+1) and FeO_2 (−1) layers. As a consequence, a built-in polarization arises within the BFO block and propagates in the opposite direction to the STO/BFO stacking (in other words, towards the substrate rather than the surface). Therefore, one can expect out-of-plane motions of the ions within this system, in order to generate an electric field which would compensate the polar discontinuity generated at the interface (and thus avoid the so-called "polar catastrophe"). This is indeed what we observe after relaxing our $(STO)_4(BFO)_2$ SL. A better stability of the system ($\Delta E = 354$ meV/*f u.*) is achieved, thanks to an elongation of the out-of-plane lattice parameter and the movement of some AO (*A* = Sr, Bi) and BO_2 (*B* = Ti, Fe) planes along the [001] direction (phase *II*, see Fig. 2(b)[18]), while a deformation of the BO_6 octahedra is induced by the off-centering of the B cation (especially

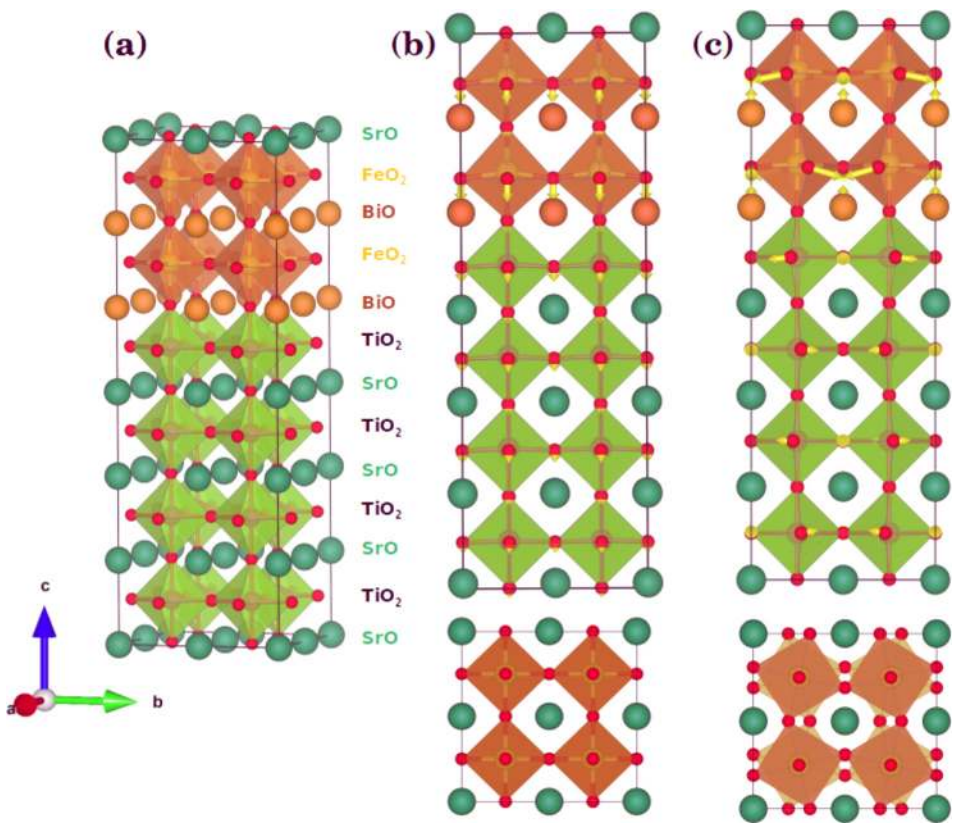

FIG. 2. (a) Representation of the $(STO)_4(BFO)_2$ unit cell used for the calculations, labelled as Phase I before relaxation. (b) The phase II is characterized by out-of-plane displacements and off-centering of the B cations after relaxation. (c) Antiferrodistortive rotations, in addition to out-of-plane displacements, of the BO_6 octahedra as observed in the Phase III.

within the FeO_6 octahedra, see Fig. 3(a)). Symmetry analysis made using the Bilbao Crystallographic server[19,20] revealed that these off-center displacements are polar. In order to estimate how these distortions can affect the ferroelectricity of $(STO)_4(BFO)_2$ SLs, we calculated the spontaneous polarization using the Berry-Phase method,[21] taking the ideal perovskite $(STO)_4(BFO)_2$ structure (i.e., phase I) as reference. Our calculation for the structure II confirmed the polarization of the material and yielded a large value of 42.4 $\mu C\,cm^{-2}$ with a polarization vector exclusively aligned along the [001] direction.

When undergoing an epitaxial strain, BFO is known to exhibit monoclinic distortions derivated from its bulk rhombohedral *R3c* structure[22–25] and phase transitions towards the *Cm*, *Pm,* or *C2/c* space groups (which lead to a progressive reorientation of the polarization vector towards the [001] direction). In addition, structural changes for perovksite compounds are regularly observed once these compounds are grown within a SL, compared to their ground state bulk structure,[26] even in the absence of strain.[27] Many cases are increasingly reported.[27–32] For example, a change in the direction of the tilt pattern for the STO was previously evidenced in a $PbTiO_3/SrTiO_3$ SL,[32] while several octahedral tilt patterns and internal symmetries have been predicted for $PbTiO_3/BiFeO_3$ superlattices at various degrees of strain.[29]

As a consequence, one can logically think that our system, as a *superlattice* undergoing an epitaxial *strain*, will exhibit similar distortions as well. In order to explore this possibility, we relaxed further our SL by allowing rotations of the BO_2 planes and octahedral tilts. We browsed a wide range of octahedral tilt patterns, supposedly compatible with the chemical nature of both constituents, among which $a^0a^0c^-$, $a^-a^-c^0$, or $a^-a^-c^-$ in the Glazer notation.[17] We also studied the hypothetical case where octahedral distortions would arise only within one block and/or both blocks having a different octahedral tilt pattern. Eventually, among all the possible combinations we have considered, a superlattice having a particular $a^0a^0c^-$ tilt pattern was found to be the most stable and lead to a an additional lowering of the energy by 107 meV/*f.u.* with respect to the structure II. The optimized structure, labelled *phase III* (see Fig. 2(c)[18]), is now characterized by antiferrodistortive rotations of the TiO_2 planes within the STO blocks. It is worth noting that this distortion scheme is comparable to the antiferrodistorsive phase developed by bulk STO under 105 K.[33] This tilt pattern propagates within the $BiFeO_3$ layers, but with a greater amplitude (see Fig. 3(b)) due to a smaller tolerance factor than $SrTiO_3$.

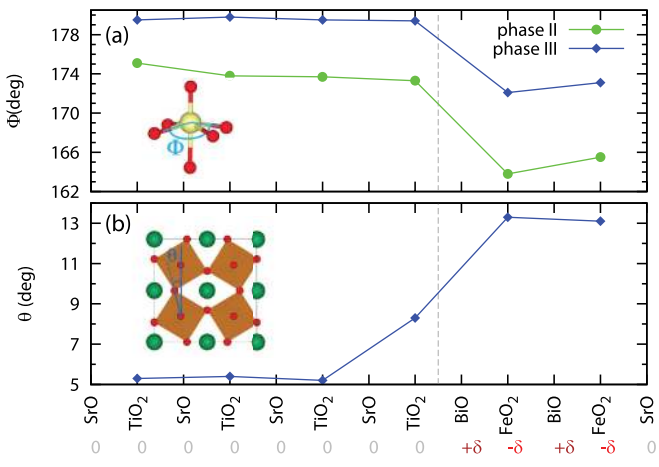

FIG. 3. Layer-by-layer resolved $\widehat{OBO}$ angle, characterizing the off-centering of B cations within the BO_6 octahedra in phase II and III (a), and octahedral rotation angle θ (b) within the phase III.

Such structural changes are governed by electrostatics and the proximity effects occurring within a superlattice. First, in such short-period SLs, oxygen ions from the BO_2 planes are surrounded by different A-site cations at each heterointerface and can therefore compensate this instability by a rotation around the Ti site within the (110) planes.[32] Another important feature is that any electric polarization, if the case, has to develop in a homogeneous way throughout the superlattice; as a consequence, structural rearrangements are needed for SL where the constituents usually exhibit, in their single crystal form, a different orientation of the polarization vector.[29] In the case of our STO/BFO SLs, the competition between the ferroelectric polarization of BFO and the different octahedral tilt patterns between STO and BFO leads to a reorientation of the polarization vector in the SL. The fact that these SLs were grown onto an STO substrate has certainly favoured the propagation of a tilt pattern similar to that of STO single crystals. The large antiferrodistorsive rotations observed in the structure III are not polar but greatly help to stabilize the material without the need of large out-of-plane displacements nor off-centerings within the octahedra with respect to the structure II (see Fig. 3(a)). As a consequence, the polarization vector has a lower amplitude than that estimated for the phase II (here, $\Delta P \sim 21.0\,\mu C.cm^{-2}$ for the phase III), but remains exclusively oriented along the [001] direction. These simulations are in agreement with the observations made by PFM imaging; moreover, we assume that the absence of in-plane component of the ferroelectric polarization contributes to a lowering of the coercive field compared to that occurring in pure BFO films, as previously observed.[5]

In summary, FE properties of $(STO)_4(BFO)_2$ SL structures were studied by means of PFM and DFT calculations. The analyses of the OP-PFM and the IP-PFM domain images confirmed that the interfacial strain present in the SL confines the FE domain orientation along the out-of-plane ⟨001⟩ direction. DFT calculation showed that this orientation is due to the tetragonal symmetry adopted by BFO in the $(STO)_4(BFO)_2$ SL. The theoretical investigation shall be now extended to a wider range of epitaxial strain; moreover, due to the antiferromagnetic nature of BFO, magnetoelectric properties can be expected in (STO)(BFO) SLs[34–36] and should be further explored.

We would like to thank the CRI of the University of Lille 1 for providing the computational facilities, A. Da Costa for his contribution in the AFM experiments, and A. Stroppa and P. Barone for very useful discussions. Chevreul institute (FR 2638), Ministère de l'Enseignement Supérieur et de la Recherche, Région Nord – Pas de Calais and FEDER are acknowledged for supporting and funding this work. Work was partly done within the frame of the LAFICS program.

[1]R. Ramesh and N. A. Spaldin, Nat. Mater. **6**, 21 (2007).
[2]G. Catalan and J. F. Scott, Adv. Mater. **21**(24), 2463 (2009).

[3]R. Ranjith, U. Lüders, W. Prellier, A. Da Costa, I. Dupont, and R. Desfeux, J. Magn. Magn. Mater. **321**, 1710 (2009).
[4]S. J. Chiu, Y. T. Liu, H. Y. Lee, G. P. Yu, and J. H. Huang, Thin Solid Films **539**, 75 (2013).
[5]R. Ranjith, R. V. K. Mangalam, Ph. Boullay, A. David, M. B. Lepetit, U. Lüders, W. Prellier, A. Da Costa, A. Ferri, R. Desfeux, Gy. Vincze, Zs. Radi, and C. Aruta, Appl. Phys. Lett. **96**, 022902 (2010).
[6]A. Ferri, A. Da Costa, R. Desfeux, M. Detalle, G. S. Wang, and D. Rèmiens, Integr. Ferroelectr. **91**, 80 (2007).
[7]C. J. M. Daumont, S. Farokhipoor, A. Ferri, J. C. Wojdel, J. Íñiguez, B. J. Kooi, and B. Noheda, Phys. Rev. B **81**, 144115 (2010).
[8]Y. Zhou, H. K. Chan, C. H. Lam, and F. G. Shin, J. Appl. Phys. **98**, 024111 (2005).
[9]M. B. Okatan and S. P. Alpay, Appl. Phys. Lett. **95**, 092902 (2009).
[10]J. Chen, Y. Luo, X. Ou, G. Yuan, Y. Wang, Y. Yang, J. Yin, and Z. Liu, J. Appl. Phys. **113**, 204105 (2013).
[11]H. Lu, C.-W. Bark, D. E. de los Ojos, J. Alcala, C. B. Eom, G. Catalan, and A. Gruverman, Science **336**, 59 (2012).
[12]Y. Luo, X. Li, L. Chang, W. Gao, G. Yuan, J. Yin, and Z. Liu, AIP Adv. **3**, 122101 (2013).
[13]A. Gruverman, A. Kholkin, A. Kingon, and H. Tokumoto, Appl. Phys. Lett. **78**, 2751 (2001).
[14]G. Kresse and J. Furthmüller, Phys. Rev. B **54**, 11169 (1996); G. Kresse and D. Joubert, *ibid*. **59**, 1758 (1999).
[15]P. E. Blochl, Phys. Rev. B **50**, 17953 (1994).
[16]J. B. Neaton, C. Ederer, U. V. Waghmare, N. A. Spaldin, and K. M. Rabe, Phys. Rev. B **71**, 014113 (2005).
[17]A. M. Glazer, Acta Crystallogr. B **28**, 3384 (1972); Acta Crystallogr. A **31**, 756 (1975).
[18]The arrows depicted here take into account the octahedral tilt as well as the out-of-plane displacement of some AO and BO_2 layers, which leads to the inclination of some vectors along the ***c***-axis. However, there is no way in which the BO_6 octahedra rotate along the *a* and/or *b* axis (this is further confirmed by the absence of any lateral shift from the apical oxygen ions).
[19]M. I. Aroyo, J. M. Perez-Mato, C. Capillas, E. Kroumova, S. Ivantchev, G. Madariaga, A. Kirov, and H. Wondratschek, "Bilbao Crystallographic Server I: Databases and crystallographic computing programs," Z. Krist. **221**(1), 15–27 (2006).
[20]M. I. Aroyo, A. Kirov, C. Capillas, J. M. Perez-Mato, and H. Wondratschek, Acta Cryst. **A62**, 115–128 (2006).
[21]R. Resta, Ferroelectrics **136**(1), 51 (1992); R. D. King-Smith and D. Vanderbilt, Phys. Rev. B **47**(3), 1651 (1993).
[22]O. Diéguez, O. E. González-Vázquez, J. C. Wojdel, and J. Íñiguez, Phys. Rev. B **83**, 094105 (2011).
[23]A. J. Hatt, N. A. Spaldin, and C. Ederer, Phys. Rev B **81**, 054109 (2010).
[24]R. J. Zeches, M. D. Rossell, J. X. Zhang, A. J. Hatt, Q. He, C.-H. Yang, A. Kumar, C. H. Wang, A. Melville, C. Adamo, G. Sheng, Y.-H. Chu, J. F. Ihlefeld, R. Erni, C. Ederer, V. Gopalan, L. Q. Chen, D. G. Schlom, N. A. Spaldin, L. W. Martin, and R. Ramesh, Science **326**, 977 (2009).
[25]H. Liu, P. Yang, K. Yao, K. P. Ong, P. Wu, and J. Wang, Adv. Funct. Mater. **22**, 937 (2012).
[26]J. M. Rondinelli and N. A. Spaldin, Adv Mater. **23**, 3363 (2011).
[27]J. M. Rondinelli and N. A. Spaldin, Phys. Rev. B **82**, 113402 (2010).
[28]J. M. Rondinelli and N. A. Spaldin, Phys. Rev. B **81**, 085109 (2010).
[29]Y. Yang, M. Stengel, W. Ren, X. H. Yan, and L. Bellaiche, Phys. Rev. B **86**, 144114 (2012).
[30]T. Saha-Dasgupta, J. Phys.: Condens. Matter **26**, 193201 (2014).
[31]X. Z. Lu, X. G. Gong, and H. J. Xiang, Comput. Mater. Sci. **91**, 310 (2014).
[32]E. Bousquet, M. Dawber, N. Stucki, C. Lichtensteiger, P. Hermet, S. Gariglio, J.-M. Triscone, and P. Ghosez, Nat. Lett. **452**, 732 (2008).
[33]H. Unoki and T. Sakudo, J. Phys. Soc. Jpn. **23**(3), 546 (1967).
[34]M. Lorenz, G. Wagner, V. Lazenka, P. Schwinkendorf, H. Modarresi, M. J. Van Bael, A. Vantomme, K. Temst, O. Oeckler, and M. Grundmann, Appl. Phys. Lett. **106**, 012905 (2015).
[35]Z. Zanolli, J. C. Wojdeł, J. Íñiguez, and P. Ghosez, Phys. Rev. B **88**, 060102(R) (2013).
[36]S. Singh, J. T. Haraldsen, J. Xiong, E. M. Choi, P. Lu, X.-D. Wen, J. Liu, H. Wang, Z. Bi, P. Yu, M. R. Fitzsimmons, J. L. MacManus-Driscoll, R. Ramesh, A. V. Balatsky, J.-X. Zhu, and Q. X. Jia, Phys. Rev. Lett **113**, 047204 (2014).